JOURNAL OF MATERIALS SCIENCE 27 (1992) 5509–5515

Development of an empirical model for subgrain growth in Al–0.6Fe alloy, aluminium, copper and nickel during recovery

MING-WEI TSENG, S. K. VARMA
Department of Metallurgical and Materials Engineering, The University of Texas at El Paso, El Paso, TX 79968, USA

Subgrain growth taking place during the recovery period of a static annealing process has been studied in Al–0.6Fe alloy, pure aluminium, nickel and copper. The kinetics of subgrain growth has been investigated at eight different temperatures for each of these materials. The slope of the curves in the graphs between the square of the subgrain diameter, D^2, and annealing time, t, at different temperatures do not agree with the calculated values from the existing models. Thus an equation has been developed to relate the experimental values of the slopes of such curves to various temperatures in each case. The fit between the experimentally observed and theoretically calculated slopes from the proposed model appears to be quite good for Al–0.6Fe alloy and pure aluminium. However, the fit is poor for nickel and copper even though the differences between the two values based on the calculation from existing theories have been minimized.

1. Introduction

The mechanical properties, such as flow stress, hardness and ductility, of metals and alloys recover monotonically towards the values characteristic of the fully annealed state during the static annealing process. Obviously the cells, developed during the deformation prior to the annealing process, grow in size during the recovery stage and presumably set the stage for eventual recrystallization events in the metal or the alloy. Thus the kinetics of recovery in terms of subgrain growth becomes a very critical area which may need a better understanding in order to control the industrially important process of static annealing.

A model presented by Sandstrom [1, 2] for the recovery of dislocations, leading to a subgrain growth process, in the subgrain interiors and sub-boundaries during static annealing, can be described by the following equation

$$D^2 = d^2 + Kt \quad (1)$$

where D is the subgrain size developed after annealing the metal at a given temperature for time, t, d is the subgrain size in the cold-worked condition, and K is a temperature-dependent constant. This treatment of subgrain growth is somewhat similar to the model presented by Li [3, 4] in the early sixties. Even though Equation 1 was tested by Sandstrom *et al.* [5] in pure aluminium and Al–1% Mn alloy for its validity, and the authors confirmed that the subgrain-boundary migration was the dominating mechanism at higher recovery temperatures, the subgrain-boundary coalescence was the controlling factor at higher recovery temperatures for subgrain growth. One of the present authors (SKV) has applied the above equation to pure aluminium [6–8], its dilute soluble [9] and insoluble [10–12] alloys, copper [13, 14] and nickel [15, 16]. The value of K obtained from the slope of the line drawn in the graph between D^2 and t was correlated with the theoretical K values in each case. In most cases the experimental K values were found to be higher than the calculated K values from Sandstrom's model.

An attempt [10, 13, 15, 16] has been made to close the gap between the calculated and theoretical K values by incorporating the movement of dislocations by the pipe diffusion mechanism [17–20] to the bulk diffusion mechanism included in Sandstrom's model. However, the differences in the K values still remain quite high. Thus the purpose of the present work was to develop an empirical equation to describe the kinetics of subgrain growth during static recovery in Al–0.6Fe alloy and pure aluminium, copper and nickel.

2. Experimental procedure

The purity of Al–0.6Fe alloy [11], pure aluminium [21], copper [22] and nickel [16] has been listed in Tables I–IV. The cold-drawn wires of these materials with prior true wire-drawing strains of 1.7, 2.09, 2.25 and 2.09 in Al–0.6Fe alloy, aluminium, nickel and copper, respectively, were subjected to a static annealing process in separate salt baths. The samples were heated for varying times at a given temperature and then immediately quenched in water at room temperature. The exact temperatures of annealing in

0022–2461

TABLE I Spectrographic analysis of Al–0.06Fe alloy (wt%)

Fe	Cr	Ni	Ga	Mg	Zn	Cu	Mn	Ti	Si	V	Al
0.064	< 0.001	< 0.001	< 0.001	< 0.001	< 0.003	< 0.001	< 0.001	< 0.001	< 0.003	< 0.001	Bal.

TABLE II Spectrographic analysis of aluminium (atomic parts per million by weight)

Li	Na	Ca	Fe	B	Si	V	Cu	C	S	Cr	Ga	O	Cl	Mn	Zn
0.01	0.04	0.02	10.00	0.80	30.00	0.07	0.02	20.00	0.50	1.00	7.00	20.00	2.00	3.00	4.00

TABLE III Spectrographic analysis of nickel (wt%)

O	Cu	Si	N	Fe	Ti	Co	Mg	V	Cr	Mn	Zr
0.0014	< 0.0005	< 0.0005	< 0.0005	< 0.0005	< 0.0005	< 0.0005	< 0.0005	< 0.0005	< 0.0005	< 0.0005	< 0.0005

TABLE IV Spark source spectrometric analysis of copper (atomic parts per million by weight)

O	C	Fe	Ag	Sb	Pb	S	As	N	Si
22.00	9.00	1.50	1.20	0.73	0.70	0.68	0.64	8.00	0.38

each case were as follows: Al–0.6Fe alloy 150, 170, 190, 200, 210, 230, 270 and 290 °C; aluminium, 150, 170, 190, 200, 210, 230, 270 and 290 °C; nickel, 200, 220, 240, 260, 280, 300, 320 and 340 °C; copper, 100, 120, 140, 150, 160, 170, 180 and 200 °C. The annealing temperatures were selected mainly on the basis of studying the kinetics of subgrain growth of these materials within reasonable periods of annealing time and still be able to compare our results with those already existing in the literature. We do, however, realize that a common homologous temperature could have been more meaningful.

The microstructural evaluations were carried out on the short cross-sections of these wires using a scanning transmission electron microscope (STEM) operating at 200 kV. The techniques of TEM sample preparation for Al–0.6Fe alloy [10], aluminium [7], copper [13] and nickel [16] have been described elsewhere. However, it must be noted that at least six samples for each heat-treated condition for a given material were analysed in the TEM for the measurement of subgrain size by the linear intercept method. A minimum of 500 intercepts were used for a given subgrain diameter measurement and the mean intercept lengths were multiplied by 1.68 to obtain the subgrain diameters.

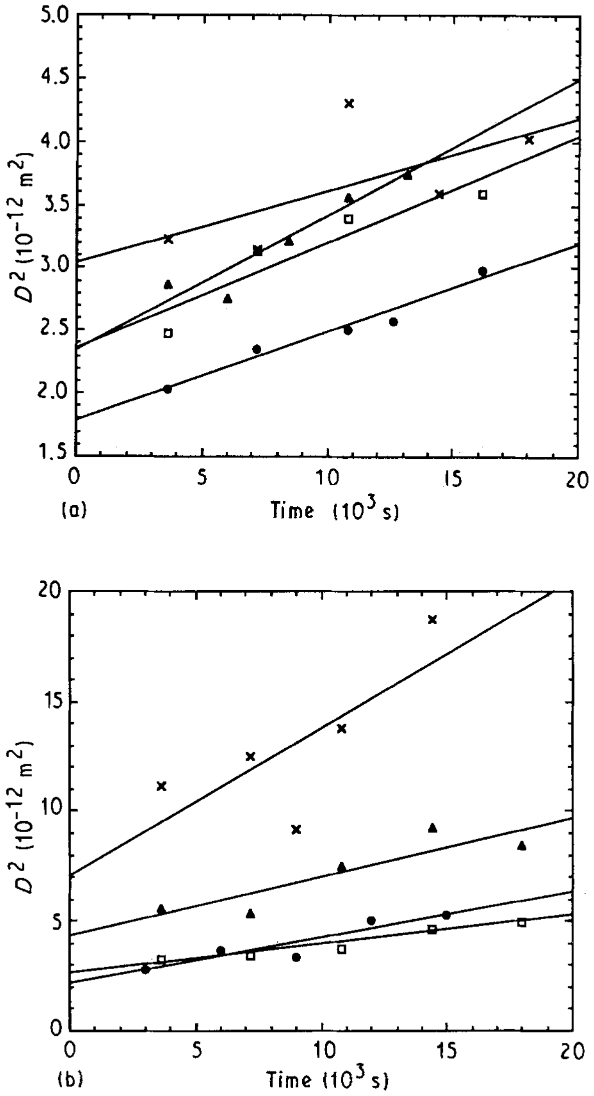

Figure 1 Variation of the square of subgrain diameter with annealing time at different temperatures in Al–0.6Fe alloy [10], (a) (●) 150 °C, (□) 170 °C, (▲) 190 °C, (×) 200 °C; (b) (●) 210 °C, (□) 230 °C, (▲) 270 °C, (×) 290 °C.

3. Results and discussion

Figs 1–4 show the variation of the square of subgrain diameter as a function of annealing time, according to Equation 1, in the temperature range indicated above for each material. The data have been fitted with a linear curve by the use of a linear regression analysis. It must be noted that the slopes of these lines in each case do not necessarily follow a given trend with respect to the annealing temperature. The cross-overs of the isotherms in these figures are, perhaps, indicative of changes in the mechanisms of subgrain growth as a function of temperature. For this reason alone, the slopes (experimental K values) have been plotted as a function of annealing temperature in Figs 5–8.

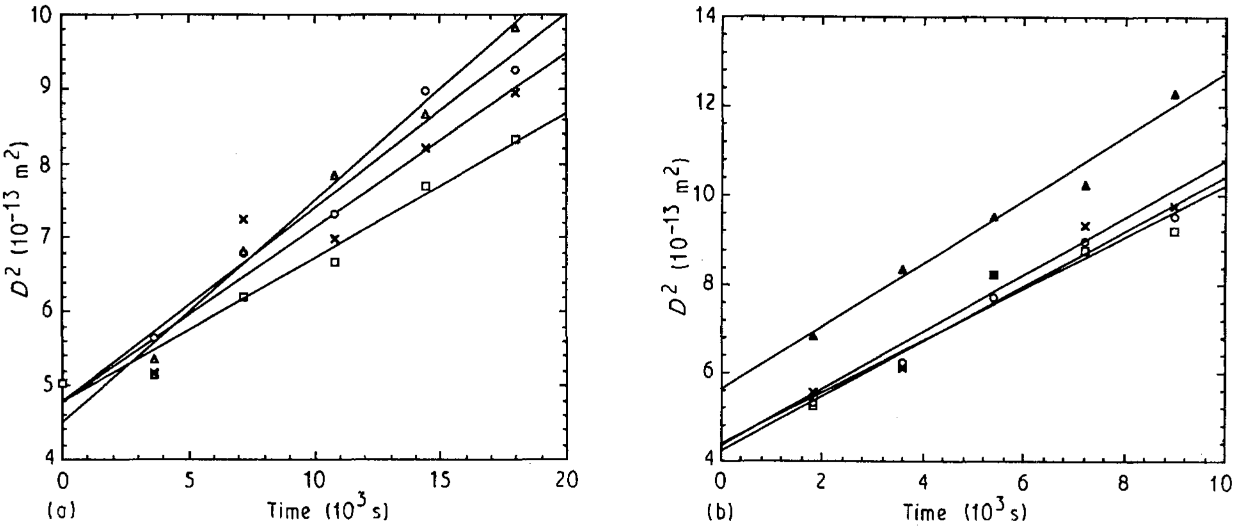

Figure 2 Variation of the square of subgrain diameter with annealing time at different temperatures in aluminium. (a) (□) 150 °C, (×) 170 °C, (○) 190 °C, (△) 200 °C; (b) (□) 210 °C, (○) 230 °C, (×) 270 °C, (▲) 290 °C.

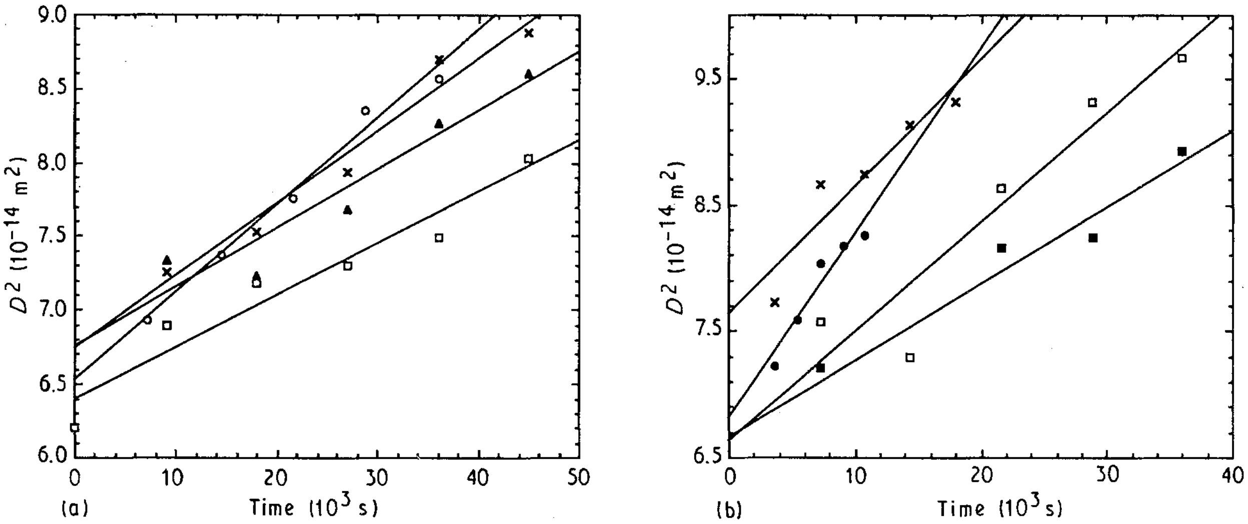

Figure 3 Variation of the square of subgrain diameter with annealing time at different temperatures in nickel. (a) (□) 200 °C, (▲) 220 °C, (×) 240 °C, (○) 260 °C; (b) (■) 280 °C, (□) 300 °C, (×) 320 °C, (●) 340 °C.

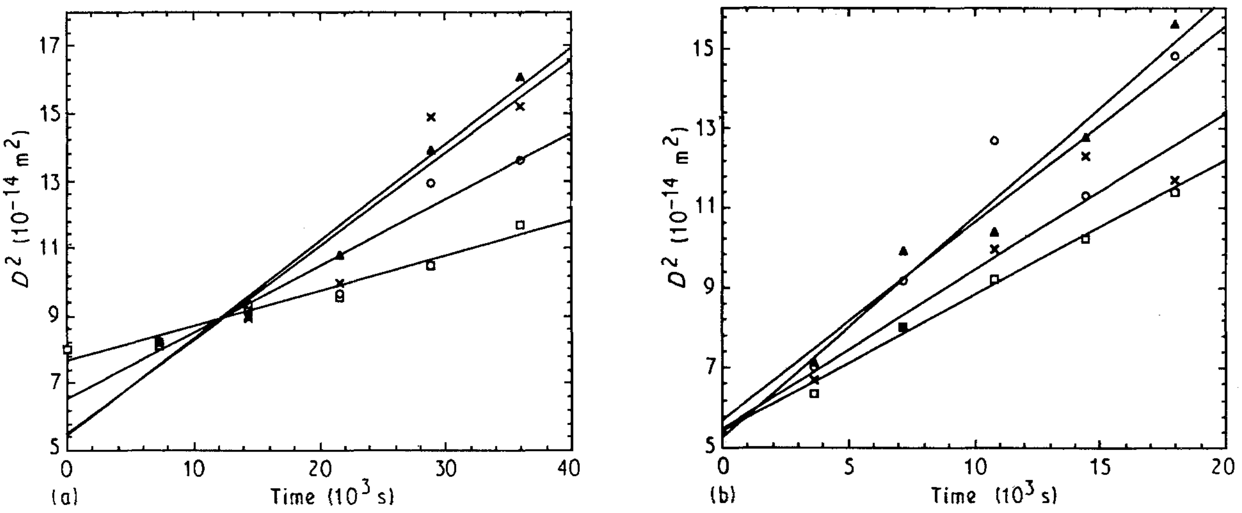

Figure 4 Variation of the square of subgrain diameter with annealing time at different temperatures in copper. (a) (□) 100 °C, (○) 120 °C, (×) 140 °C, (▲) 150 °C; (b) (□) 160 °C, (×) 170 °C, (○) 180 °C, (▲) 200 °C.

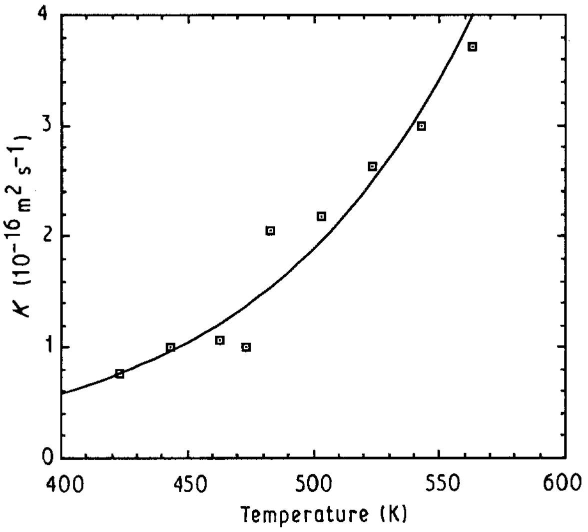

Figure 5 Variation of experimentally observed K values with annealing temperature in Al–0.6Fe alloy [10].

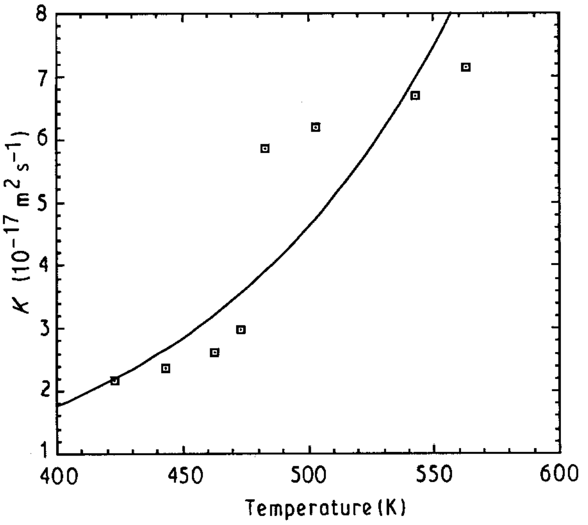

Figure 6 Variation of experimentally observed K values with annealing temperature in aluminium.

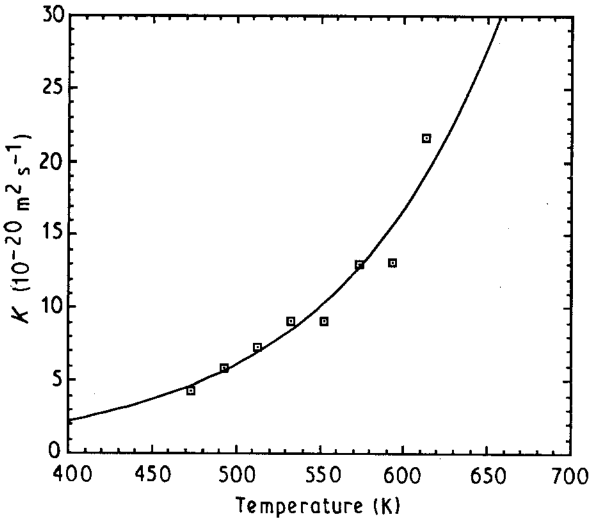

Figure 7 Variation of experimentally observed K values with annealing temperature in nickel

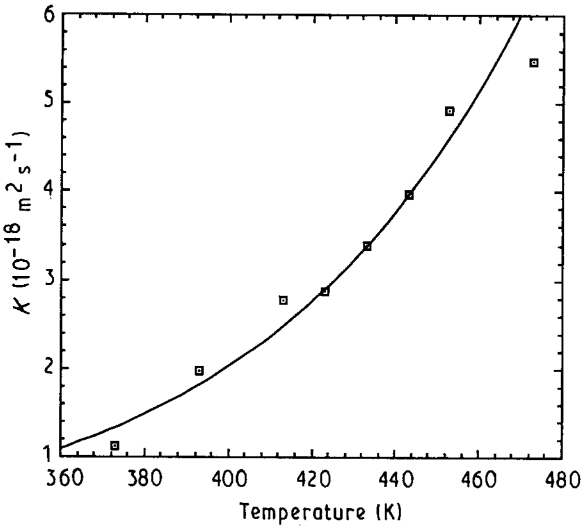

Figure 8 Variation of experimentally observed K values with annealing temperature in copper.

One of the striking features of the variation of K with t is the sudden jump of K values around a temperature of 475 K in both aluminium and Al–0.6Fe alloy. Figs 5–8 clearly show that the variation of K with temperature is such that K increases monotonically with temperature, except in the case of aluminium and Al–0.6Fe alloy at the temperature mentioned above.

The K values can be calculated from Sandstrom's model according to a procedure which will now be described in detail. The calculation of K values from Sandstrom's model involves the assumption that the subgrain growth takes place by both boundary migration and coalescence processes and their relative contributions are additive in the manner described below.

$$K_1 \text{ (for boundary coalescence alone)} = 8M\tau \quad (2)$$

$$K_2 \text{ (for boundary migration alone} = 3M\tau \quad (3)$$

so that

$$K = K_1 + K_2 = 11M\tau \quad (4)$$

where M is the dislocation mobility and τ is the dislocation line tension. These two parameters can be calculated from the following equations

$$\tau = (G\boldsymbol{b}^2/3.5) \quad (5)$$

and

$$M = (D\boldsymbol{b}/kT) \quad (6)$$

$$D = D_0 \exp(-Q/RT) \quad (7)$$

where G is the shear modulus, $\boldsymbol{b}$ Burgers vector, k Boltzmann's constant, T the annealing temperature in absolute degrees, Q the activation energy based on bulk diffusion, R the universal gas constant, D the self diffusivity, and D_0 the temperature-independent diffusion constant. From Equations 2–7, K can be calculated as

$$K = (11G\boldsymbol{b}^3D_0)/[3.5\,kT\exp(-Q/RT)] \quad (8)$$

Figs 9–12 show the variation of calculated K value from Sandstrom's model as a function of annealing time. A glance at the numbers on the K-axis in these

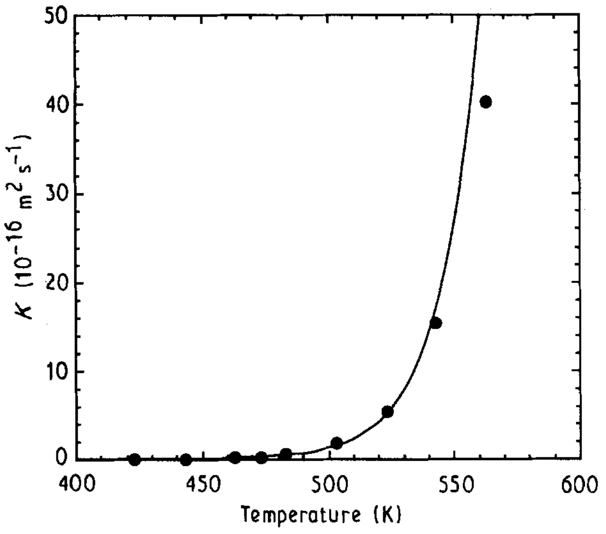

Figure 9 Variation of theoretically calculated K values from Sandstrom's model with annealing temperature in Al–0.6Fe alloy [10].

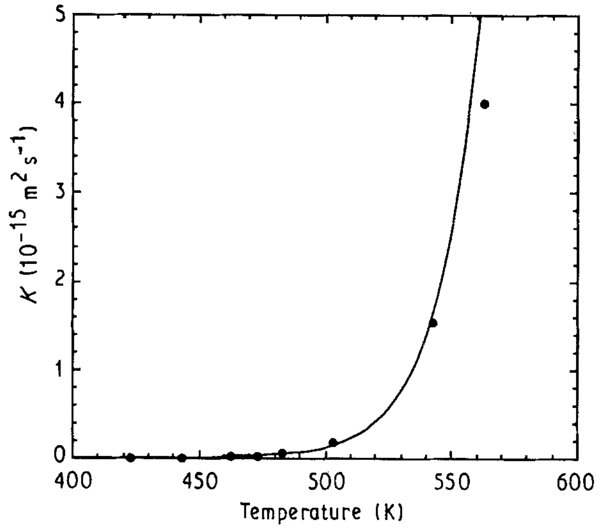

Figure 10 Variation of theoretically calculated K values from Sandstrom's model with annealing temperature in aluminium.

figures is more than enough to notice the large differences between the observed (Figs 5–8), and theoretically calculated K values from Sandstrom's model. These substantial differences imply that one or more detailed mechanisms for subgrain growth have not been explored in these metals and alloys.

Kreisler and Doherty [23] have pointed out that the mechanisms of coalescence would be dominating if the misorientation angles for the subgrains are large, while boundary migration would be dominating if the distribution of subgrain sizes shows a large non-uniformity based on the driving force in each case. For pipe diffusion, a much faster rate of coalescence was predicted to take into account the fact that the dislocations in a recovered cell structure cannot exist in isolation but can be a part of dislocation loops. The climb mobility of the dislocations can be determined from atomic diffusion across the loop. For bulk diffusion, the result is very close to that calculated by Li [3], though without the need for the very high jog density assumed in the original treatment.

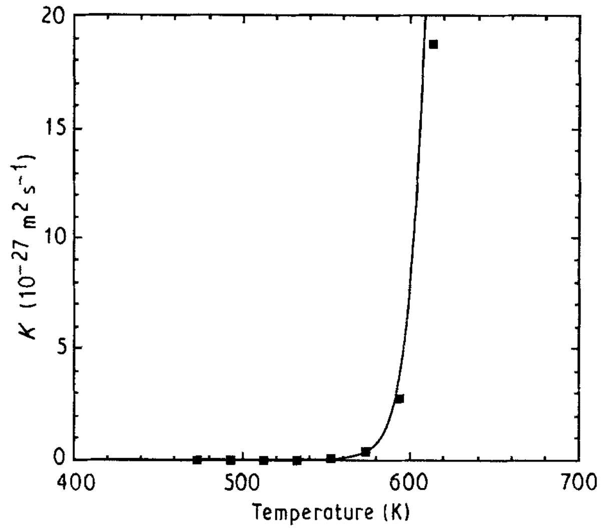

Figure 11 Variation of theoretically calculated K values from Sandstrom's model with annealing temperature in nickel.

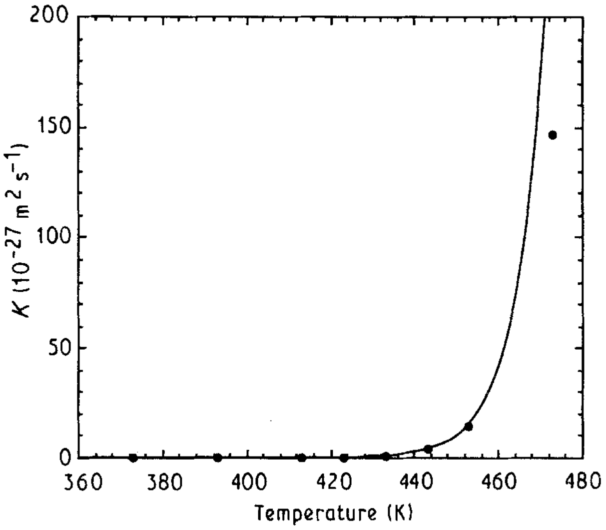

Figure 12 Variation of theoretically calculated K values from Sandstrom's model with annealing temperature in copper.

Thus by considering the experimentally measured K values in this study and taking into account the pipe diffusion mechanism for subgrain growth in addition to Sandstrom's model, we find that a better agreement between these two K values can be reached. We propose an empirical model which assumes that the K values for subgrain growth for Al–0.6Fe alloy and pure metals aluminium, nickel and copper can be obtained from the following equation

$$K_{\text{model}} = K(A\,10^{BT_{\text{m}}/T}) \qquad (9)$$

where A and B are considered to be material constants, T_{m} is the melting point of the material, K is the calculated value from Sandstrom's model and K_{model} is the proposed K value. The values of A and B, from the proposed model, for different materials of this study are reported in Table V. The comparisons between the experimental and the calculated K values based on the proposed model are shown in Figs 13–16. It is not very difficult to see that the large differences

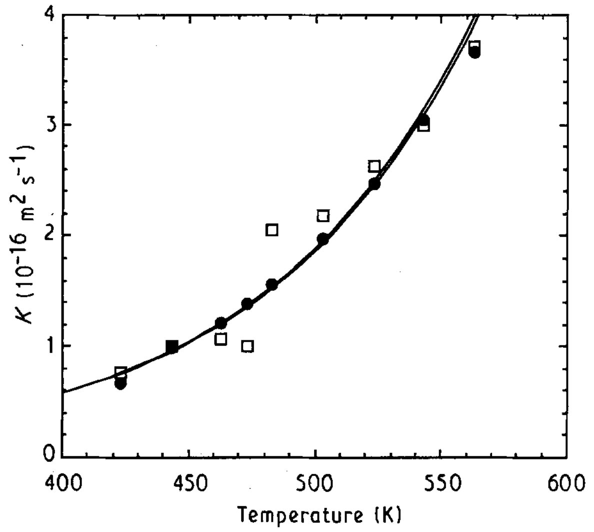

Figure 13 Comparison between the (□) experimentally observed and (●) theoretically calculated K values from the proposed empirical model in Al–0.6Fe alloy.

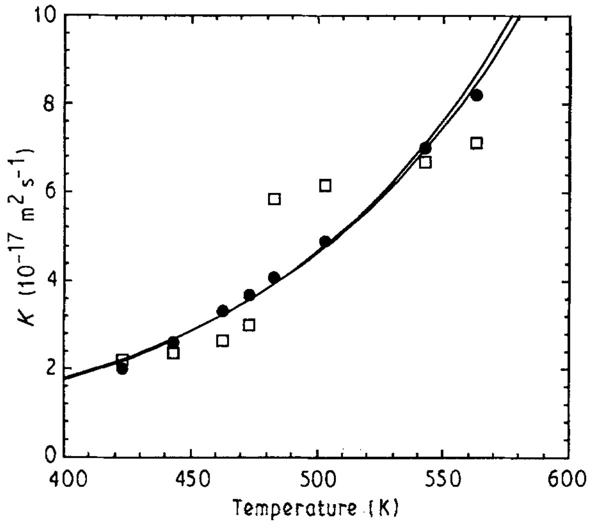

Figure 14 Comparison between the (□) experimentally observed and (●) theoretically calculated K values from the proposed empirical model in aluminium.

TABLE V Values of A and B for Al–0.6Fe alloy, aluminium, nickel and copper

Material	A	B
Al–0.6Fe	5.93×10^{-11}	5.54
Aluminium	5.60×10^{-12}	5.57
Nickel	1.00×10^{-12}	8.13
Copper	1.52×10^{-8}	5.54

between the experimental and theoretical K values have been minimized by the proposed model.

It should be noted that the proposed model is strictly empirical in nature. The only purpose for the development of Equation 9 was to show that this equation adequately fits the experimental data for subgrain growth during the static recovery process in Al–0.6Fe alloy and pure metals aluminium, nickel and copper. Because it is expected that the detailed mechanisms of these processes differ for these materials, the constants in Equation 9 must also differ.

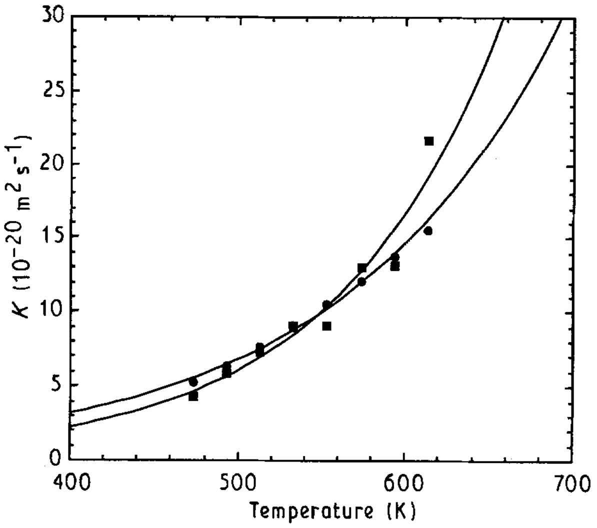

Figure 15 Comparison between the (■) experimentally observed and (●) theoretically calculated K values from the proposed empirical model in nickel.

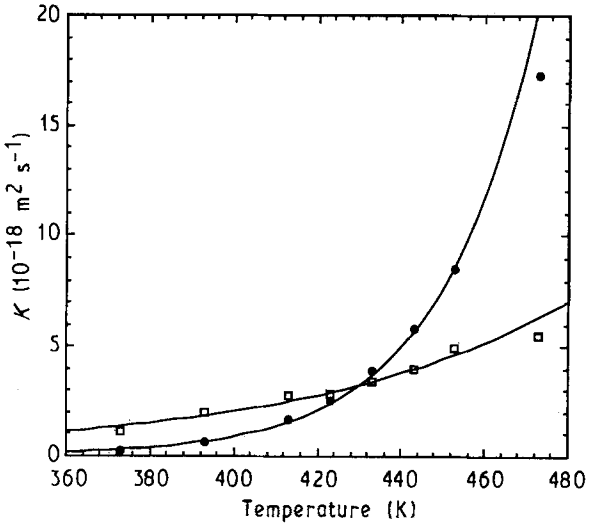

Figure 16 Comparison between the (□) experimentally observed and (●) theoretically calculated K values from the proposed empirical model in copper.

Acknowledgement

The authors thank the Texas Higher Education Coordinating Board for the financial support for this research through the grant number 003661-018.

References

1. R. SANDSTROM, *Acta Metall.* **25** (1977) 897.
2. *Idem, ibid.* **25** (1977) 905.
3. J. C. M. LI, *J. Appl. Phys.* **33** (1962) 2958.
4. *Idem*, in "Recrystallization, Grain Growth and Textures" (ASM, Metals Park, OH, 1962) p. 86.
5. R. SANDSTRÖM, B. LEHTINEN, E. HEDMAN, I. GROZA and S. KARLSSON, *J. Mater. Sci.* **13** (1978) 1229.
6. S. K. VARMA and B. C. WESSTROM, *J. Mater. Sci. Lett.* **7** (1988) 1092.

7. S. K. VARMA and B. L. WILLITS, *Metall. Trans.* **15A** (1984) 1502.
8. S. K. VARMA, *Scripta Metall.* **13** (1979) 345.
9. *Idem, Mater. Sci. Engng.* **82** (1986) L119.
10. MING-WEI TSENG and S. K. VARMA, *Scripta Metall.* **24** (1990) 1741.
11. S. K. VARMA and S. J. REYES, *Mater. Sci. Engng* **95** (1987) L1.
12. S. K. VARMA and R. W. GUARD, *J. Mater. Sci. Lett.* **5** (1986) 205.
13. CHUNG-MIN CHANG and S. K. VARMA, *Acta Metall.* **37** (1989) 927.
14. CHUNG-MIN CHANG, J. R. SERRANO and S. K. VARMA, *Mater. Sci. Engng.* **100** (1988) L15.
15. HONG ZHU and S. K. VARMA, *J. Mater. Sci. Lett.* **10** (1991) 875.
16. *Idem, Metall. Trans.* **21A** (1990) 500.
17. R. D. DOHERTY and J. A. SZPUNAR, *Acta Metall.* **32** (1984) 1789.
18. R. D. DOHERTY, *Metal Sci.* **8** (1974) 132.
19. P. FAIVRE and R. D. DOHERTY, *J. Mater. Sci.* **14** (1979) 897.
20. R. D. DOHERTY and R. W. CAHN, *J. Less-Common Metals* **28** (1972) 279.
21. I. SAMAJDAR and S. K. VARMA, *Mater. Sci. Engng.*, **A141** (1991) L1.
22. S. THIAGARAJAN and S. K. VARMA, *Metall. Trans.* **22A** (1991) 258.
23. A. KREISLER and R. D. DOHERTY, *Metal. Sci.* **12** (1978) 560.

Received 20 June 1991
and accepted 7 February 1992